ACS APPLIED MATERIALS & INTERFACES

Research Article

www.acsami.org

Direct Resonant Coupling of Al Surface Plasmon for Ultraviolet Photoluminescence Enhancement of ZnO Microrods

Junfeng Lu,[†] Jitao Li,[†] Chunxiang Xu,*[,†] Yu Li,[‡] Jun Dai,[†] Yueyue Wang,[†] Yi Lin,[†] and Shufeng Wang[‡]

[†]State Key Laboratory of Bioelectronics, School of Biological Science & Medical Engineering, Southeast University, Nanjing 210096, China

[‡]Institute of Modern Optics & State Key Laboratory for Mesoscopic Physics, School of Physics, Peking University, Beijing 100871, China

ABSTRACT: More than 170-fold ultraviolet emission enhancement was obtained from the hexagonal ZnO microrods synthesized by a simple vapor-phase transport process and decorated by Al nanoparticles (NPs). Based on the stable and transient photoluminescence (PL) spectra of the ZnO microrods sputtered with Al NPs for different times, the underlying mechanism was deduced and can be attributed to the metal surface plasmon resonance (SPR) coupling with ZnO. Interestingly, with increasing of the sputtering time, the ratio of the band gap emission to the defect-related emission was increased from 0.1 to 42.7. Our results demonstrated that ZnO microrods decorated with Al NPs shed light on developing stable and high-efficiency excitonic optoelectronic devices such as light-emitting diodes and lasers.

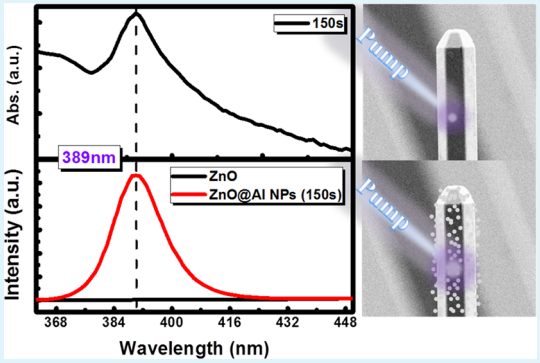

KEYWORDS: *photoluminescence, ZnO microrods, surface plasmon resonance, Al nanoparticles, vapor-phase transport*

1. INTRODUCTION

In recent years, Zinc oxide (ZnO), with a wide direct band gap (3.37 eV) and a large exciton binding energy (60 meV), has been considered as a promising candidate for efficient ultraviolet (UV) light-emitting devices (LEDs)[1,2] and low-threshold UV lasers.[3,4] To obtain highly efficient UV emission from the near band edge is one of the most important issues for photonic applications of ZnO. Surface plasmons (SPs),[5−8] excited by the interaction between light and metal surfaces, have attracted great scientific interest due to its wide applications, including plasmon lasers,[9,10] as well as enhancing the light absorption[11] and Raman scattering.[12,13] So far, a number of studies have been conducted to improve the band edge emission from ZnO films and nanostructures by using various metals. For example, Liu et al.[14] reported 12-fold enhancement of the bandgap emission from ZnO thin films by nanopatterned Pt. Coincidentally, Lin et al.[15] found that the bandgap emission of the ZnO nanorods can be greatly enhanced by employing SPs of Pt nanoparticles (NPs) and the PL intensity ratio between the bandgap and defect-related emission can be improved by up to 10^3 times. In addition, 6-fold enhancement in the near band gap emission of ZnO nanorods decorated with Au NPs had been observed by Cheng et al.,[16] while the defect-related emission was completely suppressed. Simultaneously, Niu et al.[17] achieved 11-fold enhancement of the near band emission (NBE) of the ZnO nanobelts sputtered with Au NPs. In order to reduce costs, silver has been an alternative for plasmonic materials. Recently, Cheng et al.[18] observed 3-fold enhancement of the near band emission of ZnO films by coupling through localized surface plasmons of Ag islands sputtered onto the ZnO films. Then, Liu et al.[19] fabricated UV enhanced LED by embedding a ZnO nanorod array/p-GaN film heterostructure into an Ag-NPs/PMMA composite, and the EL component from ZnO excitons was selectively enhanced more than 13-fold. However, the extinction spectra of these plasmonic materials are all in the visible range, while the NBE of ZnO is in the UV range, which will hinder the effectively resonant coupling between SP of metals and excitons of ZnO. So, it is a significant to seek a kind of metals that own the extinction spectrum matches with the NBE of ZnO. On the other hand, noble metals are always costly, which definitely restricts the potential for commercialization.

Taking advantage of the low cost and its abundance in the world, the aluminum (Al) element has now been an important candidate of plasmonic material. Especially, ε', the real part of the dielectric function, is negative even at wavelength smaller than 200 nm where ε'', the imaginary part, is still relatively low in the UV range.[20] Therefore, Al is a better plasmonic material than either Au or Ag in the blue and UV range. Based on the advantages mentioned above, Al has been used in plasmonic systems in the UV-blue spectral region, such as LSPR,[21] surface plasmon polaritons (SPPs) propagation,[22] surface-enhanced fluorescence,[23] and Raman spectroscopy.[24]

In this paper, the PL properties of the bare and Al-decorated ZnO microrods have been studied. More than 170-fold

Received: August 14, 2014
Accepted: September 22, 2014
Published: September 22, 2014

enhancement of the spontaneous emission from Al-decorated ZnO microrods was observed, while the defect-related emission was relatively suppressed effectively. On the other hand, the intensity ratio of the band gap emission to the defect-related emission increased with increasing of the sputtering time. In addition, the band edge PL decay also became fast after Al decoration. A possible mechanism of the excitons coupling with the metal SP was discussed. The results presented here would provide a great opportunity for the creation of highly efficient optoelectronic devices.

2. EXPERIMENTAL SECTION

The wurtzite-structural ZnO microrods were produced through a simple vapor-phase transport process similar to our previous report.[25] The Al NPs were sputtered onto the ZnO microrods by a radio frequency magnetic sputtering system. In order to compare the optical properties before and after decoration of Al NPs, the whole piece of Si substrate with ZnO microrods was cut into four pieces and then sputtered Al for 0, 50, 150, and 300 s, respectively. The chamber pressure is fixed at 2.0 Pa, the Ar flow is 50 sccm and the sputtering power is 100 W. The morphology and structure of the as-synthesized products were characterized by X-ray diffraction (XRD-7000, Shimadzu) using Cu Kα radiation (λ = 0.15406 nm) and a field emission scanning electron microscopy (FESEM, Carl Zeiss Ultra Plus) equipped with an X-ray energy dispersive spectrometer (EDS) (Oxford X-Max 50). The absorption measurement was carried out by UV−vis-NIR spectrophotometer (Cary-5000, Varian). The PL spectrum from the ZnO microrods was measured by a fluorescence spectrophotometer (F-4600, Hitachi) with a Xe lamp at 325 nm as the excitation source. Time-resolved photoluminescence (TRPL) experiments were performed by an optically triggered streak camera system (C10910, Hamamatsu) at 295 nm from frequency doubling of the fundamental 35 fs pulses at 590 nm with a repetition rate of 1 kHz (OperA Solo, Coherent). All measurements were performed at room temperature.

3. RESULTS AND DISCUSSION

3.1. Morphology and Structural Characterization. Figure 1a shows a typical SEM image of the ZnO microrods grown on a Si substrate. The length of the ZnO microrods is ~2 mm, and the diameter is ~10 μm. From the enlarged SEM image of the top of the microrods, a hexagonal cross section and smooth facets can be observed as inserted in Figure 1a. The EDS spectrum and elemental mapping profiles of a Al-decorated ZnO microrod confirm the existence of Al element, as shown in Figure 1(b, c). The elemental mapping images collected from the rectangular region in Figure 1b reveal that the Zn element and O element distribute uniformly corresponding to the profile of the ZnO microrod, while the Al element disperses on the surface of the ZnO microrod. Because of the same sputtering power, the diameter of the Al NPs was approximately of the same size at first. With increasing of the sputtering time, some Al NPs began to merge together. The inserted SEM images in Figure 1c further demonstrate that the diameter of the Al NPs changes from ~80 nm to ~100 nm when the sputtering time is prolonged from 50 to 300 s. Typical XRD pattern for the bare ZnO microrods is shown in Figure 1d, from which it can be seen that all the diffraction peaks of the sample match well with the indexes of the wurtzite phase of ZnO (JCPDS no. 36-1451) with the lattice constants of a = 3.250 Å and c = 5.207 Å. Furthermore, there is no other impurity peaks in the XRD pattern, and the strongest diffraction peak corresponds to the (002) diffraction plane meaning that the microrods mainly grow along the preferred [001] direction.

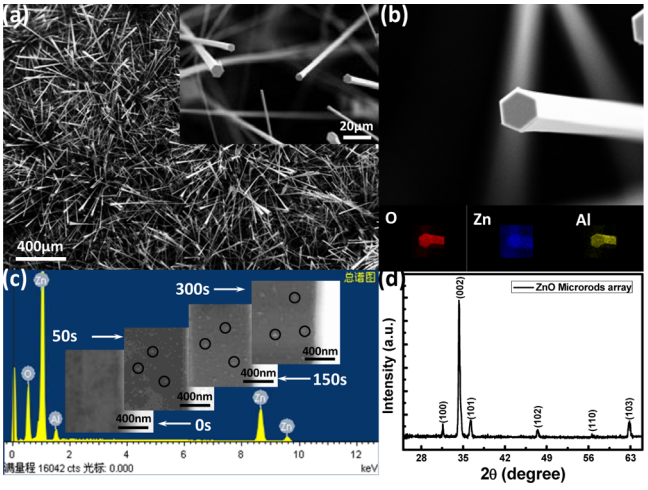

Figure 1. (a) SEM image of the as-grown ZnO microrods inserted with an enlarged top view of the microrods. (b, c) EDS spectrum and Zn, O, Al element mapping images for an individual ZnO microrod. Inset: the SEM images of the Al NPs sputtered on the surface of the ZnO microrods (0 s, 50 s, 150 s, and 300 s) deposited on the surface of the individual ZnO microrod. (d) X-ray diffraction pattern of the ZnO microrods.

3.2. Optical Property. To examine the optical properties of the ZnO microrods decorated with Al NPs for different times (0, 50, 150, and 300 s), the PL spectra measurements were performed. Two emission peaks can be observed in the PL spectra shown in Figure 2. The emission peak centered at 389 nm is assigned to the NBE of ZnO,[26,27] and the other one centered at 510 nm is the defect-related emission of ZnO. The optical property of the ZnO microrods has been significantly improved after sputtering with Al NPs with different times. The sample sputtered with 150 s presents the strongest NBE with more than 170 times enhancement compared the bare ZnO microrods and then decreases with further increasing of the sputtering time. From the normalized PL spectra shown in the inset of Figure 2, the defect emission of the ZnO microrods decorated with Al NPs is obviously suppressed compared with that of the bare one.

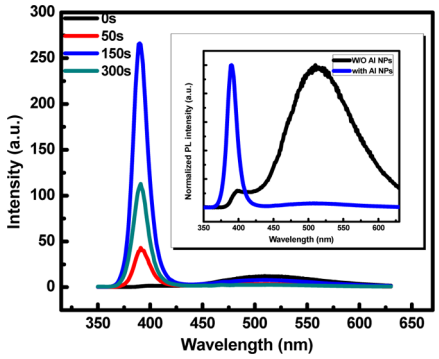

Figure 2. PL spectra of the ZnO microrods sputtered with Al NPs for different times (0, 50, 150, and 300 s). Inset: the normalized PL spectra of the two samples before and after sputtering with Al NPs (150 s).

Table 1 summarizes the peak position of the ZnO NBE and the enhancement ratio for ZnO micronano structures decorated

Table 1. Comparison of the Peak Position and Enhancement Ratio for ZnO Micro−Nano Structure Decorated with Different Kinds of Metals in This Work and Previous Reports[14−19,28]

metal	peak position (nm)	enhancement ratio	ref.
Pt	380	12	14
	380	~14	15
Au	378	6	16
	381	11	17
Ag	380	3	18
	~380	11	19
Al	375	2.5	28
	389	170	present work

with different kinds of metals in this work and previous reports.[14−19,28] Compared with the ZnO nanostructures decorated with other metals, the ZnO microrods with Al NPs decoration in the present work shows much higher enhancement ratio.

To further understand the effect of Al NPs on the ratio of the intensity of the NBE emission to the defect-related one (I_{NBE}/I_{defect}), the PL spectra of the ZnO microrods decorated with Al NPs for different times has been normalized, as shown in Figure 3a. It can be seen that I_{NBE}/I_{defect} was improved by up to 4×10^2 times with increasing of the sputtering time. In order to explain the exciting experimental phenomenon and understand the underlying mechanism, the optical absorption spectra of Al NPs with different sputtering time under the same sputtering condition was measured, as shown in Figure 3b. An obvious absorption exists in ZnO NBE region, and a red shift was observed, which can be attributed to the merging of Al NPs with increasing of sputtering time. In order to illustrate the aforementioned mechanism, the schematic diagram of the band alignment between the ZnO and Al NPs was plotted as shown in Figure 3c, in which the conduction band of ZnO is located at −4.19 eV versus the absolute vacuum scale (AVS), and the Fermi level of Al is at −4.3 eV versus AVS.[29,30] Because of the closed response of Al SPR to the ZnO interband electron transition shown in the schematic diagram, an effectively resonant energy coupling has occurred between the SPs of Al NPs and the NBE of ZnO. The SPR coupling will give rise to an enhanced interband transition and further result in an enhanced band gap recombination for spontaneous emission from ZnO microrods. Based on this mechanism, it is reasonable to deduce that more effective coupling would happen when the formant of Al NPs matched with the NBE of ZnO best. With increasing of the sputtering time, the Al NPs will merge together, which will lead to the red shift of the Al NPs' absorption peak, as that shown in the absorption spectrum. On the other hand, more defect emission from the ZnO microrods can be absorbed by the electrons in Al NPs due to the shift of the Al NPs' absorption peak in the long-wavelength region. So the value of I_{NBE}/I_{defect} for the Al NPs-decorated ZnO microrods will increase with increasing of the sputtering time.

TRPL experiments were performed to gain more insights of the coupling mechanism. Figure 4 shows the room temperature TRPL of the bare and Al-decorated ZnO microrods (with sputtering time of 150 s). The fitting of these TRPL decay curves involves a deconvolution between the instrument response function and a monoexponential radiative decay. The decay lifetime τ is defined as

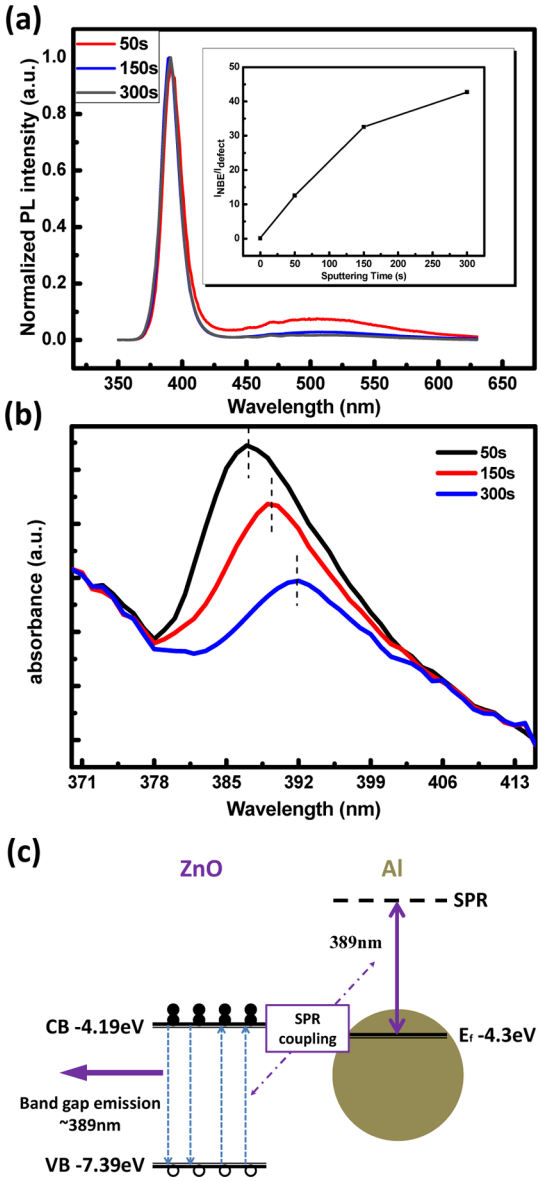

Figure 3. (a) Normalized PL spectra inserted with the value of I_{NBE}/I_{defect} for the ZnO microrods decorated with Al NPs as a function of sputtering time and (b) the absorption spectrum of the Al NPs sputtering with different times (50, 150, and 300 s). (c) Schematic resonant coupling between SPs of Al and the NBE of ZnO.

$$I(t) = I_0 \exp(-t/\tau) \quad (1)$$

where I_0 is the normalization constant. It can be calculated that the lifetime of ZnO microrods decorated with Al NPs (~0.98 ns) has been shortened compared with the bare one (~1.23 ns), which is the evidence of SP-exciton coupling. These observations are in agreement with previous reports on SPs coupling with ZnMgO films.[31] The PL decay time of bare ZnO (τ_{ZnO}) can be expressed as

$$\frac{1}{\tau_{ZnO}} = \frac{1}{\tau_{NR}} + \frac{1}{\tau_R} \quad (2)$$

where τ_{NR} and τ_R represent the nonradiative and radiative decay time of the bare ZnO, respectively. After being decorated with Al NPs, a new recombination path (SPs coupling) is created and the decay time (τ_{ZnO-Al}) can be modified as

dx.doi.org/10.1021/am505492r | ACS Appl. Mater. Interfaces 2014, 6, 18301−18305

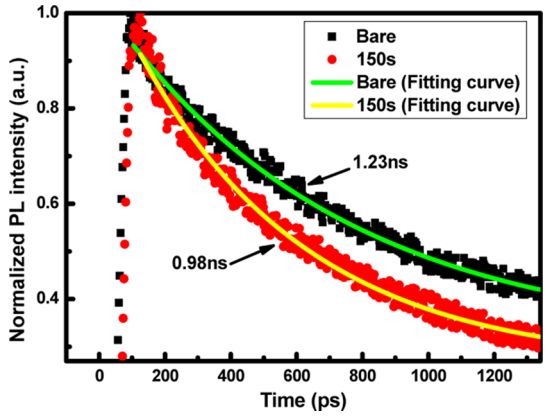

Figure 4. Representative room temperature TRPL decays of bare ZnO and Al-decorated ZnO with 150 s sputtering.

$$\frac{1}{\tau_{ZnO-Al}} = \frac{1}{\tau^*_{NR}} + \frac{1}{\tau^*_{R}} + \frac{1}{\tau_{SP}} \quad (3)$$

where τ^*_{NR} and τ^*_{R} are nonradiative and radiative decay time of Al-decorated ZnO, respectively, and τ_{SP} is the exciton-SP coupling lifetime. As τ_{SP} is expected to be very small, the spontaneous emission rate of Al-decorated ZnO microrods is faster than that of bare ZnO microrods. Based on the above results, it can be further confirmed that the direct resonant coupling occurs between the Al NPs and ZnO microrods. Combined with the results of PL measurement shown in Figure 2, we propose that there are two distinct physical processes that account for the band edge emission enhancement and the visible emission suppression, respectively. First, the enormous enhancement of the band edge emission is due to the direct resonant coupling between excitons of ZnO and SPs of Al NPs. More than 170-fold enhancement of the NBE was observed when the sputtering time of Al NPs increased to 150 s, the formant of which matched with the NBE of ZnO best. However, with the further increase of the sputtering time, the PL intensity of the band gap emission decreased, which can be attributed to the intension of the absorption, leading to the increase of the nonradiative recombination. In this case, the absorption process will dominate over the scattering so that radiation as photons into free space will be suppressed due to nonradiative dissipation of the SPs. Simultaneously, more Al NPs began to merge together with increasing of the sputtering time as shown in the inset of Figure 1c. Then, the red shift of the absorption peak will occur with increasing of the Al NPs' diameter, giving rise to the mismatch between the formant of Al NPs and the NBE of ZnO. Second, the obvious suppression of the visible emission can also be discovered along with the enhancement of the band gap emission, which can be ascribed to the red shift of the absorption peak with increasing of the sputtering time. With the merging of Al NPs, the coupling efficiency between the SPs of Al NPs and the excitons of ZnO will decrease, whereas more and more energy of the defect emission will be absorbed by the electrons from Al NPs. Subsequently, hot electrons are created in the high energy states and can transfer back to the conduction band of ZnO microrods. In other words, electrons in the defect states are pumped via Al to the conduction band of ZnO. Hence, PL intensity of the band gap emission is enhanced and in parallel the defect emission is suppressed.

4. CONCLUSION

In summary, we have shown more than 170-fold enhancement of the band edge emission of ZnO microrods by decorating Al NPs, while the defect emission of the microrods are obviously suppressed. The enhancement mechanism of the NBE emission can be ascribed to the resonant coupling between excitons of ZnO and SPs of Al NPs. TRPL results indicate that the Al NPs can effectively increase the spontaneous emission rate due to the formation of surface plasmon resonance. We believe that the SP enhancement of the band edge emission will provide a promising method for developing highly efficient photoelectric devices.

AUTHOR INFORMATION

Corresponding Author

*Email: xcxseu@seu.edu.cn.

Notes

The authors declare no competing financial interest.

ACKNOWLEDGMENTS

This work was supported by 973 Program (2011CB302004 and 2013CB932903), NSFC (61275054), MOE (20110092130006), and JSIS (BE2012164).

REFERENCES

(1) Shen, H.; Shan, C. X.; Qiao, Q.; Liu, J. S.; Lia, B. H.; Shen, D. Z. Stable Surface Plasmon Enhanced ZnO Homojunction Light-Emitting Devices. *J. Mater. Chem. C* **2013**, *1*, 234−237.

(2) Yang, Q.; Liu, Y.; Pan, C. F.; Chen, J.; Wen, X. N.; Wang, Z. L. Enhancing Light Emission of ZnO Microwire-Based Diodes by Piezo-Phototronic Effect. *Nano Lett.* **2013**, *13*, 607−613.

(3) Dai, J.; Xu, C. X.; Sun, X. W. ZnO-Microrod/p-GaN Heterostructured Whispering-Gallery-Mode Microlaser Diodes. *Adv. Mater.* **2011**, *23*, 4115−4119.

(4) Chu, S.; Wang, G. P.; Zhou, W. H.; Lin, Y. Q.; Chernyak, L.; Zhao, J. Z.; Kong, J. Y.; Li, L.; Ren, J. J.; Liu, J. L. Electrically Pumped Waveguide Lasing from ZnO Nanowires. *Nat. Nanotechnol.* **2011**, *6*, 506−510.

(5) Oulton, R. F.; Sorger, V. J.; Genov, D. A.; Pile, D. F. P.; Zhang, X. A Hybrid Plasmonic Waveguide for Subwavelength Confinement and Long-range Propagation. *Nat. Photonics* **2008**, *2*, 496−500.

(6) Liu, R.; Fu, X. W.; Meng, J.; Bie, Y. Q.; Yu, D. P.; Liao, Z. M. Graphene Plasmon Enhanced Photoluminescence in ZnO Microwires. *Nanoscale* **2013**, *5*, 5294−5298.

(7) Hwang, S. W.; Shin, D. H.; Kim, C. O.; Hong, S. H.; Kim, M. C.; Kim, J.; Lim, K. Y.; Kim, S.; Choi, S. H.; Ahn, K. J.; Kim, G.; Sim, S. H.; Hong, B. H. Plasmon-Enhanced Ultraviolet Photoluminescence from Hybrid Structures of Graphene/ZnO Films. *Phys. Rev. Lett.* **2010**, *105*, 127403.

(8) Lin, Y.; Xu, C. X.; Li, J. T.; Zhu, G. Y.; Xu, X. Y.; Dai, J.; Wang, B. P. Localized Surface Plasmon Resonance-Enhanced Two-Photon Excited Ultraviolet Emission of Au-Decorated ZnO Nanorod Arrays. *Adv. Opt. Mater.* **2013**, *1*, 940−945.

(9) Sorger, V. J.; Zhang, X. Spotlight on Plasmon Lasers. *Science* **2011**, *333*, 709−710.

(10) Lu, Y. J.; Kim, J.; Chen, H. Y.; Wu, C.; Dabidian, N.; Sanders, C. E.; Wang, C. Y.; Lu, M. Y.; Li, B. H.; Qiu, X. G.; Chang, W. H.; Chen, L. J.; Shvets, G.; Shih, C. K.; Gwo, S. Plasmonic Nanolaser Using Epitaxially Grown Silver Film. *Science* **2012**, *337*, 450−453.

(11) Schaadt, D. M.; Feng, B.; Yub, E. T. Enhanced Semiconductor Optical Absorption via Surface Plasmon Excitation in Metal Nanoparticles. *Appl. Phys. Lett.* **2005**, *86*, 063106.

(12) Nie, S. M.; Emory, S. R. Probing Single Molecules and Single Nanoparticles by Surface-Enhanced Raman Scattering. *Science* **1997**, *275*, 1102−1106.

(13) Campion, A.; Kambhampati, P. Surface-Enhanced Raman Scattering. *Chem. Soc. Rev.* **1998**, *27*, 241−250.
(14) Liu, K. W.; Tang, Y. D.; Cong, C. X.; Sum, T. C.; Huan, A. C. H.; Shen, Z. X.; Wang, L.; Jiang, F. Y.; Sun, X. W.; Sun, H. D. Giant Enhancement of Top Emission from ZnO Thin Film by Nano-patterned Pt. *Appl. Phys. Lett.* **2009**, *94*, 151102.
(15) Lin, J. M.; Lin, H. Y.; Cheng, C. L.; Chen, Y. F. Giant Enhancement of Bandgap Emission of ZnO Nanorods by Platinum Nanoparticles. *Nanotechnology* **2006**, *17*, 4391−4394.
(16) Cheng, C. W.; Sie, E. J.; Liu, B.; Huan, C. H. A.; Sum, T. C.; Sun, H. D.; Fana, H. J. Surface Plasmon Enhanced Band Edge Luminescence of ZnO Nanorods by Capping Au Nanoparticles. *Appl. Phys. Lett.* **2010**, *96*, 071107.
(17) Niu, B. J.; Wu, L. L.; Tang, W.; Zhang, X. T.; Meng, Q. G. Enhancement of Near-Band Edge Emission of Au/ZnO Composite Nanobelts by Surface Plasmon Resonance. *CrystEngComm* **2011**, *13*, 3678−3681.
(18) Cheng, P. H.; Li, D. S.; Yuan, Z. Z.; Chen, P. L.; Yang, D. R. Enhancement of ZnO Light Emission via Coupling with Localized Surface Plasmon of Ag Island Film. *Appl. Phys. Lett.* **2008**, *92*, 041119.
(19) Liu, W. Z.; Xu, H. Y.; Wang, C. L.; Zhang, L. X.; Zhang, C.; Sun, S. Y.; Ma, J. G.; Zhang, X. T.; Wang, J. N.; Liu, Y. C. Enhanced Ultraviolet Emission and Improved Spatial Distribution Uniformity of ZnO Nanorod Array Light-Emitting Diodes via Ag Nanoparticles Decoration. *Nanoscale* **2013**, *5*, 8634−8639.
(20) West, P. R.; Ishii, S.; Naik, G. V.; Emani, N. K.; Shalaev, V. M.; Boltasseva, A. Searching for Better Plasmonic Materials. *Laser Photonics Rev.* **2010**, *4*, 795−808.
(21) Langhammer, C.; Schwind, M.; Kasemo, B.; Zoric, I. Localized Surface Plasmon Resonances in Aluminum Nanodisks. *Nano Lett.* **2008**, *8*, 1461−1471.
(22) Quail, J. C.; Rako, J. G.; Simon, H. J. Long-Range Surface-Plasmon Modes in Silver and Aluminum Films. *Opt. Lett.* **1983**, *8*, 377−379.
(23) Ray, K.; Chowdhury, M. H.; Lakowicz, J. R. Aluminum Nanostructured Films as Substrates for Enhanced Fluorescence in the Ultraviolet-Blue Spectral Region. *Anal. Chem.* **2007**, *79*, 6480−6487.
(24) Taguchi, A.; Hayazawa, N.; Furusawa, K.; Ishitobi, H.; Kawata, S. Deep-UV Tip-Enhanced Raman Scattering. *J. Raman Spectrosc.* **2009**, *40*, 1324−1330.
(25) Zhu, G. P.; Xu, C. X.; Zhu, J.; Lv, C. G.; Cui, Y. P. Two-Photon Excited Whispering-Gallery Mode Ultraviolet Laser from an Individual ZnO Microneedle. *Appl. Phys. Lett.* **2009**, *94*, 051106.
(26) Zhang, N.; Tang, W.; Wang, P.; Zhang, X. T.; Zhao, Z. Y. In Situ Enhancement of NBE Emission of Au−ZnO Composite Nanowires by SPR. *CrystEngComm* **2013**, *15*, 3301−3304.
(27) Xu, X. Y.; Xu, C. X.; Lin, Y.; Ding, T.; Fang, S. J.; Shi, Z. L.; Xia, W. W.; Hu, J. G. Surface Photoluminescence and Magnetism in Hydrothermally Grown Undoped ZnO Nanorod Arrays. *Appl. Phys. Lett.* **2012**, *100*, 172401.
(28) Wu, K. W.; Lu, Y. F.; He, H. P.; Huang, J. Y.; Zhao, B. H.; Ye, Z. Z. Enhanced Near Band Edge Emission of ZnO via Surface Plasmon Resonance of Aluminum Nanoparticles. *J. Appl. Phys.* **2011**, *110*, 023510.
(29) Michaelson, H. B. The Work Function of the Elements and Its Periodicity. *J. Appl. Phys.* **1977**, *48*, 4729−4733.
(30) Skriver, H. L.; Rosengaard, N. M. Surface Energy and Work Function of Elemental Metals. *Phys. Rev. B* **1992**, *46*, 7157−7168.
(31) Wang, Y. J.; He, H. P.; Zhang, Y. L.; Sun, L. W.; Hu, L.; Wu, K. W.; Huang, J. Y.; Ye, Z. Z. Metal Enhanced Photoluminescence from Al-Capped ZnMgO Films: The Roles of Plasmonic Coupling and Non-Radiative Recombination. *Appl. Phys. Lett.* **2012**, *100*, 112103.